Crystal structure of *Drosophila* angiotensin I-converting enzyme bound to captopril and lisinopril[1]

Ho Min Kim[a], Dong Ryeol Shin[b], Ook Joon Yoo[a,c], Hayyoung Lee[d], Jie-Oh Lee[b,*]

[a] *Department of Biological Science, Korea Advanced Institute of Science and Technology, 373-1 Kusong-dong, Yusong-gu, Daejeon, South Korea*
[b] *Department of Chemistry, Korea Advanced Institute of Science and Technology, 373-1 Kusong-dong, Yusong-gu, Daejeon, South Korea*
[c] *Biomedical Research Center, Korea Advanced Institute of Science and Technology, 373-1 Kusong-dong, Yusong-gu, Daejeon, South Korea*
[d] *Center for Biotechnology, Chungnam National University, Daejeon, South Korea*

Received 7 January 2003; revised 23 January 2003; accepted 24 January 2003

First published online 12 February 2003

Edited by Hans Eklund

Abstract Angiotensin I-converting enzymes (ACEs) are zinc metallopeptidases that cleave carboxy-terminal dipeptides from short peptide hormones. We have determined the crystal structures of AnCE, a *Drosophila* homolog of ACE, with and without bound inhibitors to 2.4 Å resolution. AnCE contains a large internal channel encompassing the entire protein molecule. This substrate-binding channel is composed of two chambers, reminiscent of a peanut shell. The inhibitor and zinc-binding sites are located in the narrow bottleneck connecting the two chambers. The substrate and inhibitor specificity of AnCE appears to be determined by extensive hydrogen-bonding networks and ionic interactions in the active site channel. The catalytically important zinc ion is coordinated by the conserved Glu395 and histidine residues from a HExxH motif.

Key words: Angiotensin I-converting enzyme; Angiotensin; Captopril; Lisinopril; X-ray crystal structure

1. Introduction

Angiotensin I-converting enzyme (ACE) is a zinc metallopeptidase that cleaves a C-terminal dipeptide. ACE plays an important role in regulating blood pressure maintenance and heart function by catalyzing the production of the hypertensive peptide, angiotensin II, as well as the destruction of the hypotensive peptide, bradykinin [1,2]. Specific inhibitors of ACE such as captopril and lisinopril are highly effective as antihypertensive drugs and are widely used in the clinic [3,4]. Two types of human ACE are known. The somatic form of ACE contains two homologous domains of about 600 amino acids; both domains contain an intact zinc-binding site critical for catalysis [5]. However, the testicular form of human ACE contains only one domain that is essentially identical to the C-terminal domain of somatic ACE [6,7]. ACEs are an evolutionarily conserved family of proteins. Two *Drosophila* homologs of ACE, AnCE and Acer, have been reported [8–11]. The *Drosophila* ACEs contain a single ACE domain, similar to the testicular form of human ACE. The sequence identity between human testicular ACE and *Drosophila* AnCE is 42% overall and reaches higher than 70% in the regions surrounding the enzyme active site [8,9]. AnCE can hydrolyze angiotensin I and many of the other known substrates of human ACE [12,13]. The activity of AnCE is inhibited by various inhibitors of human ACE with high potency [12,14]. These data suggest that the catalytic mechanism and structure of the enzyme are conserved in the *Drosophila* AnCE. The catalytic mechanism of ACE has been proposed based on that of thermolysin, a zinc metallopeptidase, because they share a HExxH zinc-binding motif [15,16]. However, other than this short peptide motif, the sequence homology of ACE with other zinc proteases is minimal, and the exact molecular mechanism of ACE action has not been clearly identified. We have determined the crystal structure of AnCE, with and without the inhibitors captopril and lisinopril.

2. Materials and methods

Complementary DNA of *Drosophila* AnCE (residues 1–615) was obtained from a *Drosophila* QuickClone cDNA library (Clontech) using the polymerase chain reaction, and was confirmed by DNA sequencing. AnCE cDNA, tagged with six histidine codons at the C-terminus, was cloned into the pVL1393 baculovirus transfer vector (Pharmingen). The hexahistidine-tagged AnCE fusion protein was secreted into the culture medium of Hi5 cells (Clontech) after virus infection. The culture medium was harvested after 2 days of viral infection. The secreted AnCE was purified using TALON metal affinity chromatography (Clontech), Source-Q anion exchange and Superdex-200 gel filtration chromatography (Amersham Pharmacia Biotech). The purified protein was concentrated to 20–25 mg/ml in a buffer containing 20 mM HEPES, 0.2 M NaCl (pH 7.5). Crystals were grown at 22°C, using the hanging-drop vapor diffusion method, by mixing 2 μl of the protein solution and 2 μl of crystallization buffer containing 7.2 M sodium formate, 2 mM $ZnCl_2$. The crystals containing bound inhibitors were grown with an additional 2 mM of captopril or lisinopril added to the protein solution. Crystals suitable for diffraction experiments were obtained after 1 week.

Data from AnCE crystals containing lisinopril or captopril were collected at the Cornell High Energy Synchrotron Source in Ithaca, NY, USA, on the A1 beamline using the ADSC Quantum 4 detector at $\lambda = 0.9280$ Å. The native and heavy atom derivative data were collected using a rotating-anode X-ray generator and an R-AXIS IV detector. Intensities were integrated, reduced, scaled and post-refined with the HKL package (HKL Research). The crystals belong to $P2_1$ space group with unit dimensions $a = 94.5$ Å, $b = 121.3$ Å, $c = 94.5$ Å and $\beta = 99.1°$. The crystallographic asymmetric unit contains two protein molecules. Data collection statistics are summarized in Table 1.

*Corresponding author. Fax: (82)-42-869 5839.
E-mail address: jieoh@kaist.ac.kr (J.-O. Lee).

[1] Atomic coordinates (codes 1J36, 1J37 and 1J38) have been deposited in the Protein Data Bank.

Abbreviations: ACE, angiotensin I-converting enzyme; NCS, non-crystallographic symmetry

0014-5793/03/$22.00 © 2003 Published by Elsevier Science B.V. on behalf of the Federation of European Biochemical Societies.
doi:10.1016/S0014-5793(03)00128-5

The native structure without a bound inhibitor was determined by MIR procedures using the SOLVE 2.03 program [17]. The initial phases were significantly improved by two-fold non-crystallographic symmetry (NCS) averaging, solvent flattening and histogram matching, using the RESOLVE 2.03 program [17]. Most α-helices could be automatically traced by the RESOLVE 2.03 and Refmac 5.0 [18]. The resulting electron density map showed clear densities for most of the backbone and side chains and the majority of the side chain atoms were built in the first round of manual modeling using program O [19]. Errors in the initial modeling were corrected in the subsequent simulated annealed refinement and manual remodeling using the CNS [20] and O programs. The NCS-related atoms were tightly restrained throughout the refinement process, except during the last cycle. The refined structure without a bound inhibitor was used as an initial model for refinement with data from crystals containing captopril or lisinopril. The partially refined F_o-F_c difference Fourier electron density map showed clear densities for the inhibitor molecules lisinopril and captopril. The atomic coordinates for lisinopril and captopril were obtained from the Cambridge Structural Database. The flexible torsion angles of lisinopril were manually adjusted initially and then refined using the CNS program. The overall protein geometry of the final refined structure was good, with an absence of non-Gly, non-Pro residues in the disallowed regions of the Ramachandran plot.

3. Results and discussion

3.1. Structure of AnCE

The crystal structures of AnCE were determined using the multiple isomorphous replacement technique with data to 2.4 Å resolution. AnCE is 615 amino acids long and its structure is composed of 21 α-helices and three antiparallel β-strands (Fig. 1). AnCE contains a large internal channel encompassing the entire protein molecule; this highly unusual substrate-binding channel is composed of two chambers, reminiscent of a peanut shell. The zinc ion critical for catalysis is located in the narrow bottleneck connecting these two chambers.

The zinc ion is penta-coordinated by the conserved residues Glu395, His367 and His371, and two water molecules in the absence of a bound inhibitor (Fig. 2A). Mutations of these metal-coordinating residues of human somatic ACE result in complete inactivation of the enzyme, emphasizing the crucial role of zinc in catalysis [21,22]. Asp399 indirectly coordinates zinc through interaction with His367, via hydrogen bonding. Mutation of Asp399 to an alanine has a more subtle effect, reducing k_{cat} by 22-fold [22]. The zinc coordination geometry of ACE is identical with that of the gluzincin family of zinc metalloproteases, which contain the HExxH motif [16].

Captopril is a competitive inhibitor of ACE, and binds to human ACE and *Drosophila* AnCE with K_is of 1.4 and 1.1 nM, respectively [14]. Captopril mimics two carboxy-terminal residues of the enzyme substrate. The sulfhydryl group of captopril replaces the zinc-binding water molecule and directly interacts with the zinc ion, with a distorted tetrahedral geometry (Fig. 2B). The carboxy-end of the proline moiety is held by three highly conserved residues, Gln265, Lys495 and Tyr504, through ionic and hydrogen bonds. These residues probably prevent sliding of the substrate from the catalytic site in the large enzyme internal channel. This kind of locking mechanism may slip when the negative charge of the carboxy-terminus is masked by amidation. For most substrates, ACE cleaves the carboxy-terminal dipeptide, but it can hydrolyze three amino acids from substance P and luteinizing hormone-releasing hormone whose carboxy-termini are modified by amidation [1]. The sulfhydryl group and the terminal proline moieties of captopril are connected by a peptide bond. The position of the carbonyl oxygen of the peptide bond is locked by three strong hydrogen bonds with residues His337, His497 and Tyr507. Mutation of the His1089 residue of human somatic ACE, corresponding to the His497 residue of *Drosophila* AnCE, abolishes binding of captopril and lisinopril to the enzyme [23].

Lisinopril is another highly efficient inhibitor of ACE. It binds to the C-domain of human somatic ACE with a K_i of 0.2 nM and to *Drosophila* AnCE with a K_i of 18 nM [12,14]. Similar to captopril, lisinopril appears to mimic peptide substrates. The residue that mediates binding of the carboxy-terminal proline moiety of captopril is also involved in binding of the proline moiety of lisinopril (Fig. 2C). In comparison to captopril, lisinopril contains an additional lysine and a phenyl group. The lysine side chain of lisinopril makes water-mediated hydrogen bonds with residues Thr364 and Asp360. Ionic interactions with the negatively charged Asp360, Asp146 and Glu150 also enhance binding of the lysine group. Asp146 and Asp360 are conserved or replaced by glutamates in human ACEs. Similar to captopril, the His337 and His497 residues interact with the carbonyl oxygen of the peptide bond connecting the terminal proline and lysine moiety of lisinopril. The secondary amine group connecting the lysine and the amino-terminal phenyl group of lisinopril makes a strong hydrogen bond with the backbone carbonyl oxygen of Ala338. In lisinopril and related inhibitors, the carboxylic group, instead of the sulfhydryl group, mediates zinc chelation. These two carboxylic oxygens make direct coordination to zinc with penta-coordinated geometry, and appear to mimic the nucleophilic water and the carbonyl oxygen of the substrate in the tetrahedral intermediates during the enzymatic reaction. Similar penta-coordinated zinc chelation geometry is found in thermolysin bound to transition-state mimicking inhibitors (see below). The conserved Glu368 and Tyr507 side chains make close contacts with the metal-coordinating carboxylic oxygens of lisinopril. Residues directly involved in the zinc and inhibitor binding are completely conserved in the known ACE sequences (see **web supplementary data**[2]).

3.2. The substrate specificity of ACE

The substrate-binding site of AnCE is a large continuous internal channel (Fig. 3). This peanut shell-shaped channel is composed of two chambers of unequal size. The larger chamber is the binding site of the amino-terminal eight amino acids of the substrate angiotensin I, and will be referred to as the 'N-chamber' in this article. The carboxy dipeptide portion of the substrate binds to the smaller chamber, and will be referred to as the 'C-chamber'. The N- and C-chambers are 8.5 and 7.0 Å long, and 6.3 and 5.0 Å wide at their widest points, respectively. These spacious chambers are sufficiently large for the binding of short substrate peptides. However, size limitations of the internal channel prevent binding and hydrolysis of longer peptides or globular proteins. The catalytic zinc and inhibitor binding sites are located in the narrow bottleneck connecting the two chambers. The N- and C-chambers are open to the exterior solvent area through narrow holes with approximate diameters of 3 Å, which appear to be too small for the passage of peptide substrates. Flexibility and a breath-

[2] http://www.elsevier.com/locate/febs

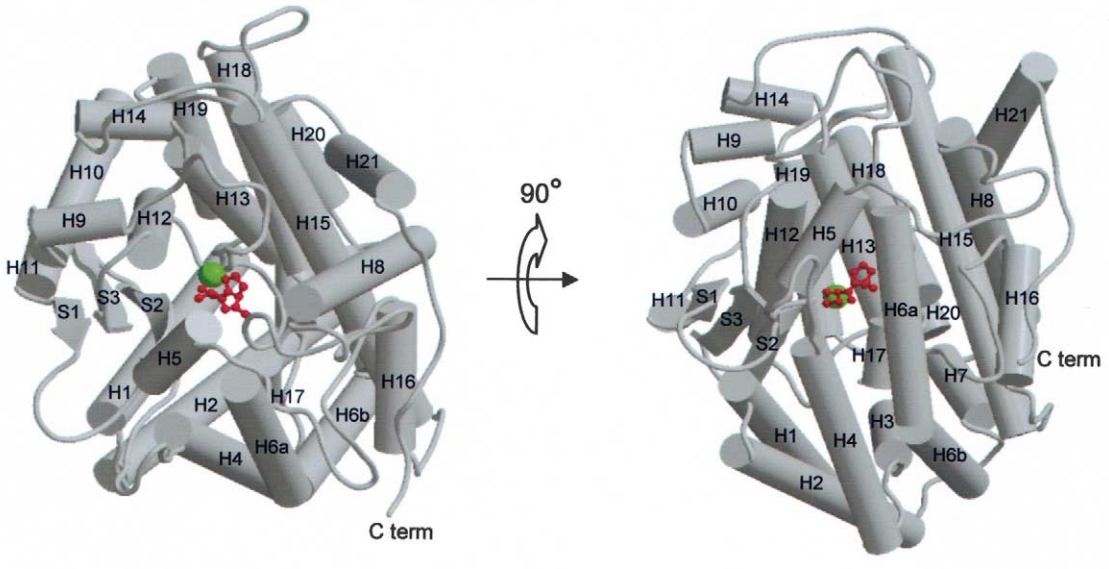

Fig. 1. Schematic diagram of the *Drosophila* AnCE structure. The zinc ion and the bound inhibitor, captopril, are shown in green and red, respectively.

ing motion of the opening holes are probably required for efficient catalysis.

The main interactions between AnCE and substrate-mimicking inhibitors are mediated by ionic and hydrogen bonds. The inhibitors cannot fill up the spacious substrate-binding channel and the shape of the inhibitors or substrates appears to have a minor role in determining specificity of the enzyme. ACE is a relatively non-specific dipeptidase. However, it has weak but noticeable tendencies in substrate selection. ACE generally favors a hydrophobic residue at the carboxy-terminus of the substrate [24]. The binding surface of the carboxy-terminal proline moieties of the inhibitors is composed of a hydrophobic patch provided by residues Phe441, Phe444, Phe511, Tyr504 and Tyr507 of AnCE. This conserved patch may be involved in the binding of bulky hydrophobic residues such as isoleucines or phenylalanines in ACE substrates. The substrate-binding channel of AnCE is predominantly negatively charged (Fig. 3). This may explain why human and *Drosophila* ACEs generally favor positively charged substrates [1,25]. Negatively charged amino acids are sometimes found at the amino-terminus but rarely in the middle of the sequences of the known ACE substrates [1,13].

Table 1
Crystallographic statistics

Diffraction data				
Data set	Native	Captopril	Lisinopril	
D_{min} (Å)	2.6	2.4	2.4	
Number of measurements	442 229	590 560	547 813	
Unique reflections	66 143	82 133	82 806	
% Complete (outer shell)	92.8 (81.7)	90.8 (76.4)	92.2 (79.6)	
I/σ (outer shell)	23.9 (6.0)	19.5 (3.0)	22.1 (4.7)	
R_{merge} (%) (outer shell)	6.3 (23.4)	5.9 (37.5)	5.4 (23.3)	
Phasing				
Derivative	Mercury chloride	Methyl mercury chloride	Trimethyl lead acetate	Lead nitrate
Concentration (mM)	5	5	10	10
Temperature (°C)	22	22	22	22
Soaking time (h)	10	2	24	48
Number of sites	7	10	6	3
Phasing power[a]	0.82	0.89	0.68	0.47
Mean figure of merit[b]		0.56		
Refinement				
Data set	Native	Captopril	Lisinopril	
Data range (Å)	20–2.6	20–2.4	20–2.4	
R factor (%)	24.6	24.1	23.4	
R_{free} factor (%)	28.1	28.3	28.0	
Rms deviations				
Bond lengths (Å)	0.008	0.009	0.009	
Bond angles (°)	1.5	1.5	1.4	
NCS-related atoms (Å)	0.028	0.029	0.022	
Mean B factors (Å^2)	22.0	26.3	23.5	
Number of protein atoms	9800	9800	9800	
Number of solvent atoms	500	600	600	

[a]Phasing power = $\langle F \rangle / E$ where $\langle F \rangle$ is the root mean square heavy atom structure factor and E is the residual lack of closure error.
[b]Figure of merit = cosine of the likely error in the phase angles.

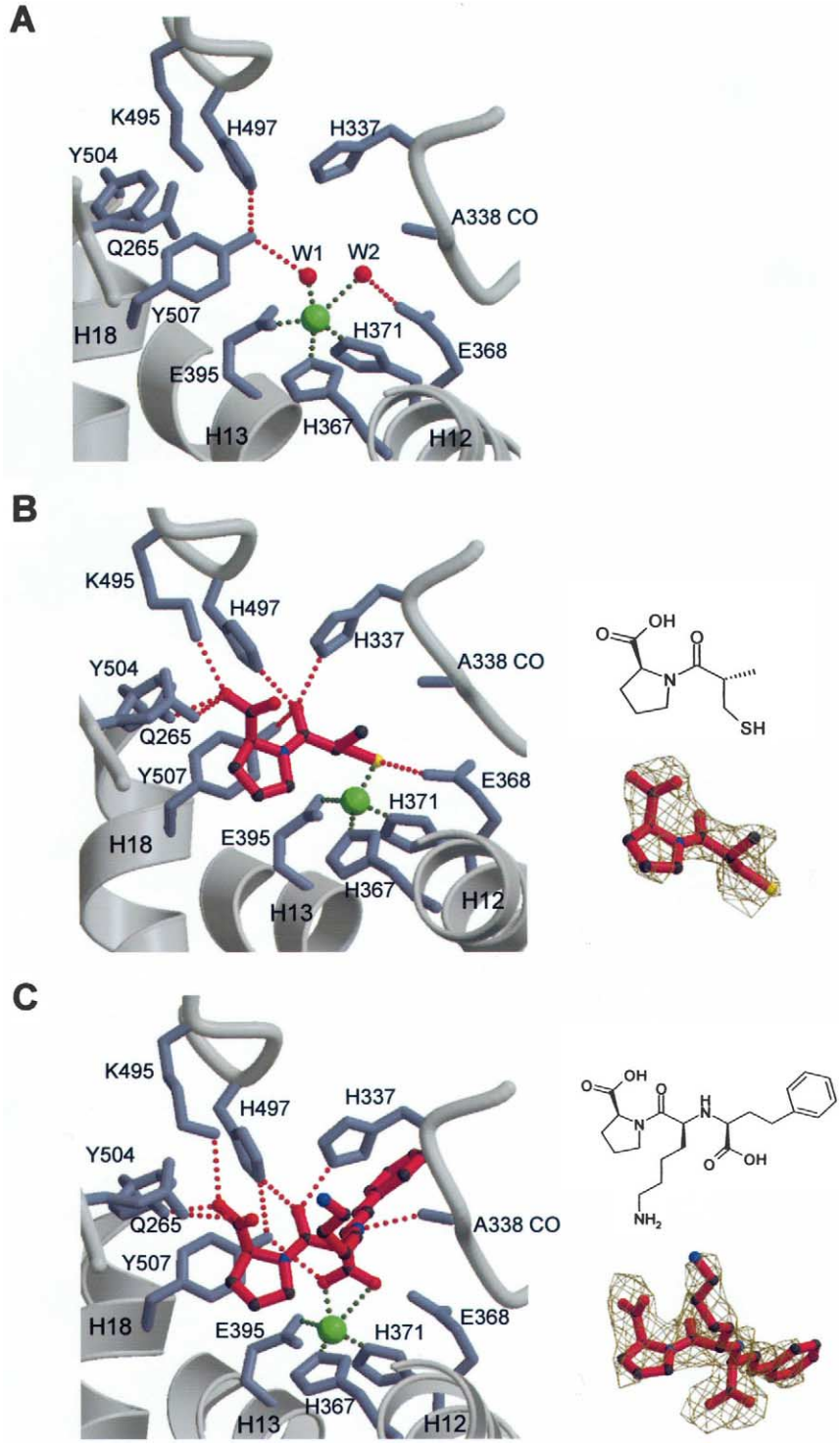

Fig. 2. Close-up view of the active site. A: The zinc ion without a bound inhibitor is penta-coordinated by conserved protein residues and two water molecules. The zinc ion and coordinating water molecules are shown as green and red balls, respectively. The potential hydrogen-bonding partners are connected by broken red lines. The broken green lines represent the metal coordination bonds. B: The active site with a bound captopril is schematically drawn in the left panel. The chemical structure of captopril is shown in the top right panel. F_o-F_c difference electron density map calculated with the protein structure refined without the inhibitor is contoured at 1.7σ and superimposed with the final refined model including captopril (bottom right panel). C: The active site with a bound lisinopril is schematically drawn in the left panel. The chemical structure of lisinopril (top right panel) and F_o-F_c difference electron density map (bottom right panel), calculated as for B, are shown.

ACE2 is a recently discovered homolog of ACE [26,27]. ACE2 shares high sequence homology with ACE. Residues Glu395, His367 and His371, coordinating zinc, or residues Glu368, Tyr507 and His497, critical for the catalysis of AnCE, are completely conserved in both ACE and ACE2 (see **web supplementary data**[2]). Surprisingly, ACE2 cleaves a single amino acid rather than a dipeptide from the substrate. The classical inhibitors of ACE, including captopril and lisi-

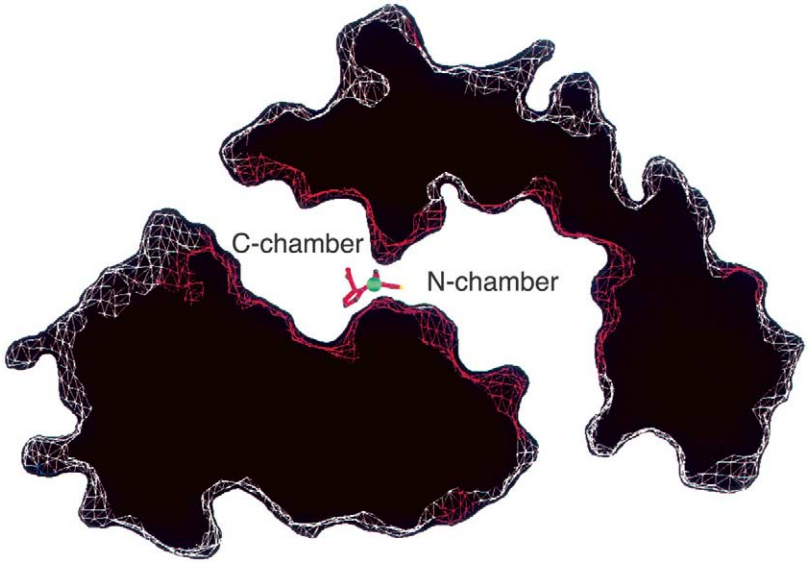

Fig. 3. Cross-sectional view of the substrate-binding channel. The view is rotated approximately 90° counterclockwise about the vertical axis of the right panel of Fig. 1. The metal ion and bound inhibitor are shown in green and red, respectively. The red and blue mesh represents negatively and positively charged surface, respectively.

nopril, do not bind to ACE2 [26,27]. To explain the remarkable differences in substrate and inhibitor specificity, we built models of human ACE and ACE2 based on our crystal structure. Homology modeling of human testicular ACE and ACE2 was performed using the program Swiss-Model [28] or Modeller6 v.2 [29]. The molecular modeling was straightforward owing to the high sequence homology, and both techniques gave essentially identical results. This study reveals two significant changes that may affect substrate binding and hydrolysis. In the AnCE structure, Gln265 makes a hydrogen bond to the terminal carboxylic group of substrate-mimicking inhibitors. This residue is changed to an arginine in ACE2 (see **web supplementary data**[2]). The long and positively charged side chain of the arginine may shift the substrate by one amino acid, and the carboxy-terminus, instead of the second terminal peptide bond, may be positioned to the catalytic site. Arg500 of ACE2, which replaces Ser510 of AnCE, is also located in close proximity to the carboxy-terminal residue and may have a similar role. In addition to these changes, residues Lys495 and Tyr504, which interact with terminal carboxylic oxygens in AnCE, are changed in ACE2.

3.3. Comparison with other zinc metallopeptidases

ACE belongs to the gluzincin family of metalloproteases [16]. Proteins of this family have minimal sequence homology apart from their conserved HExxH zinc-binding motif. The catalytic mechanism of a bacterial gluzincin, thermolysin, has been extensively studied and has served as a prototype of the HExxH-containing zinc proteases [15,16]. Other than this short zinc-binding motif, thermolysin and ACE share no sequence or structural homologies. However, the zinc coordination geometry, and some residues critical for the hydrolysis, are conserved between these two enzymes, suggesting that catalysis by ACE may proceed through a reaction mechanism

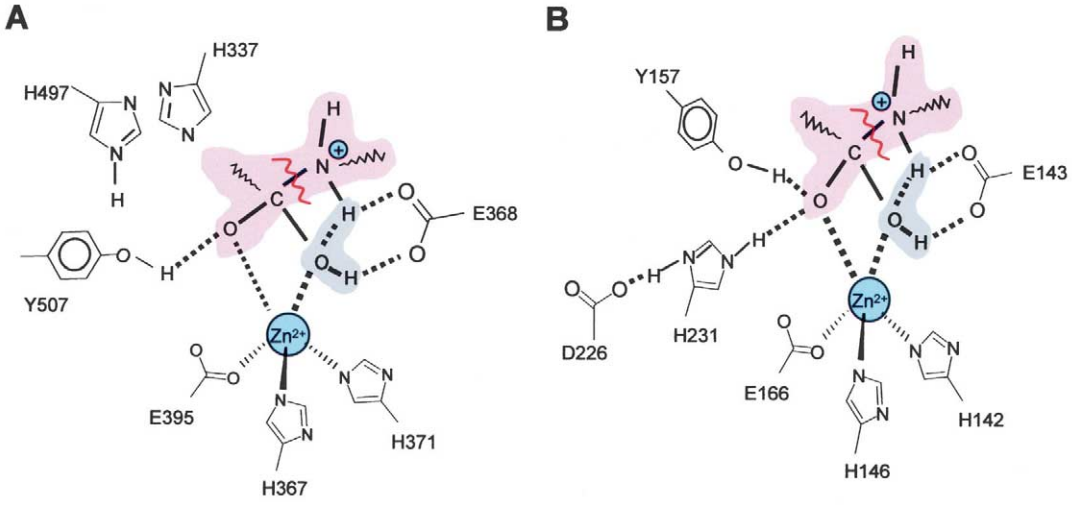

Fig. 4. Proposed reaction intermediates of AnCE (A) and thermolysin (B). His337 and His497 of AnCE are located close to Tyr507 and may have an effect on catalysis. The scissile peptide bonds are marked with curved red lines.

similar to that of thermolysin. In thermolysin, Glu143 plays a pivotal role by polarizing a nucleophilic water molecule and by shuttling protons to the substrate (Fig. 4B). Glu368 in AnCE occupies a nearly identical position and probably plays a similar role in the ACE reaction mechanism (Fig. 4A). His231 and Tyr157 residues in thermolysin are critical for the enzyme activity; they promote formation of the tetrahedral intermediate by stabilizing negative charges. In thermolysin, the acidity of His231 is enhanced by the Asp226 residue located close to His231. The position of His231 in thermolysin is occupied by Tyr507 in AnCE, which suggests that Tyr507 may have a similar role in ACE catalysis. A residue that may replace Asp226 of thermolysin is not found in the AnCE structure. Instead, the AnCE active site includes His497, which is separated by 3.3 Å from Tyr507. His497 is located more than 5 Å away from the presumed binding site of the catalytic carbonyl group of the substrate, and is unlikely to play a direct role in stabilizing the tetrahedral intermediate. Mutation of the His1089 residue of human somatic ACE, corresponding to the His497 residue of *Drosophila* AnCE, reduces the k_{cat} by 100-fold, with only a mild increase of K_m [23]. These mutation data support the hypothesis that His497 of AnCE plays a role similar to that of Asp226 in thermolysin. It requires further study to clarify the role of His497 in AnCE catalysis. Interestingly, AnCE contains an additional histidine residue, His337, near the catalytic site. His337 is highly conserved in human and *Drosophila* ACEs and is located 4 Å from His497. The interaction network formed by His337, His497 and Tyr507 in AnCE may play a role in stabilizing the transition state during catalysis.

The overall shape of AnCE resembles several other zinc metalloproteases, such as neurolysin and neprilysin, which cleave short peptide hormones [30,31]. These enzymes have their active sites in the large internal chambers that restrict entry of the larger substrates. The topology of AnCE is practically identical to that of neurolysin but is different from that of neprilysin. Therefore, AnCE and neprilysin may represent a case of convergent evolution.

4. Note added in proof

While this paper was in press, an independent crystal structure of human testicular ACE was reported [32].

Acknowledgements: The authors thank the staff at the Cornell High Energy Synchrotron Source for assistance in data collection. This study was supported by a grant of the Korea Health 21 R&D Project, Ministry of Health and Welfare, Republic of Korea (01-PJ1-PG3-20900-0029).

References

[1] Skidgel, R.A. and Erdos, E.G. (1993) in: The Renin-Angiotensin System, Vol. 1 (Robertson, J.I.S. and Nicholls, M.G., Eds.), pp. 10.1–10.10, Gower Medical, New York.
[2] Corvol, P., Williams, T.A. and Soubrier, F. (1995) Methods Enzymol. 248, 283–305.
[3] Jackson, E. and Garrison, J.C. (1996) in: The Pharmacological Basis of Therapeutics (Hardman, J.G. and Limbird, L.E., Eds.), pp. 733–758, McGraw-Hill, New York.
[4] Raia Jr., J.J., Barone, J.A., Byerly, W.G. and Lacy, C.R. (1990) Annals Pharmacotherapy 24, 506–525.
[5] Soubrier, F., Alhenc-Gelas, F., Hubert, C., Allegrini, J., John, M., Tregear, G. and Corvol, P. (1988) Proc. Natl. Acad. Sci. USA 85, 9386–9390.
[6] Lattion, A.L., Soubrier, F., Allegrini, J., Hubert, C., Corvol, P. and Alhenc-Gelas, F. (1989) FEBS Lett. 252, 99–104.
[7] Ehlers, M.R., Fox, E.A., Strydom, D.J. and Riordan, J.F. (1989) Proc. Natl. Acad. Sci. USA 86, 7741–7745.
[8] Cornell, M.J. et al. (1995) J. Biol. Chem. 270, 13613–13619.
[9] Tatei, K., Cai, H., Ip, Y.T. and Levine, M. (1995) Mech. Dev. 51, 157–168.
[10] Lamango, N.S. and Isaac, R.E. (1994) Biochem. J. 299, 651–657.
[11] Taylor, C.A., Coates, D. and Shirras, A.D. (1996) Gene 181, 191–197.
[12] Houard, X., Williams, T.A., Michaud, A., Dani, P., Isaac, R.E., Shirras, A.D., Coates, D. and Corvol, P. (1998) Eur. J. Biochem. 257, 599–606.
[13] Siviter, R.J., Nachman, R.J., Dani, M.P., Keen, J.N., Shirras, A.D. and Isaac, R.E. (2002) Peptides 23, 2025–2034.
[14] Williams, T.A., Michaud, A., Houard, X., Chauvet, M.T., Soubrier, F. and Corvol, P. (1996) Biochem. J. 318, 125–131.
[15] Pelmenschikov, V., Blomberg, M.R. and Siegbahn, P.E. (2002) J. Biol. Inorg. Chem. 7, 284–298.
[16] Lipscomb, W.N. and Strater, N. (1996) Chem. Rev. 96, 2375–2434.
[17] Terwilliger, T.C. and Berendzen, J. (1999) Acta Crystallogr. D Biol. Crystallogr. 55, 849–861.
[18] Pannu, N.S., Murshudov, G.N., Dodson, E.J. and Read, R.J. (1998) Acta Crystallogr. D Biol. Crystallogr. 54, 1285–1294.
[19] Jones, T.A., Zou, J.Y., Cowan, S.W. and Kjeldgaard, M. (1991) Acta Crystallogr. A 47, 110–119.
[20] Brunger, A.T. et al. (1998) Acta Crystallogr. D Biol. Crystallogr. 54, 905–921.
[21] Wei, L., Alhenc-Gelas, F., Corvol, P. and Clauser, E. (1991) J. Biol. Chem. 266, 9002–9008.
[22] Williams, T.A., Corvol, P. and Soubrier, F. (1994) J. Biol. Chem. 269, 29430–29434.
[23] Fernandez, M., Liu, X., Wouters, M.A., Heyberger, S. and Husain, A. (2001) J. Biol. Chem. 276, 4998–5004.
[24] Cheung, H.S., Wang, F.L., Ondetti, M.A., Sabo, E.F. and Cushman, D.W. (1980) J. Biol. Chem. 255, 401–407.
[25] Isaac, R., Schoofs, L., Williams, T.A., Veelaert, D., Sajid, M., Corvol, P. and Coates, D. (1998) Biochem. J. 330, 61–65.
[26] Donoghue, M. et al. (2000) Circ. Res. 87, E1–E9.
[27] Tipnis, S.R., Hooper, N.M., Hyde, R., Karran, E., Christie, G. and Turner, A.J. (2000) J. Biol. Chem. 275, 33238–33243.
[28] Guex, N., Diemand, A. and Peitsch, M.C. (1999) Trends Biochem. Sci. 24, 364–367.
[29] Marti-Renom, M.A., Stuart, A.C., Fiser, A., Sanchez, R., Melo, F. and Sali, A. (2000) Annu. Rev. Biophys. Biomol. Struct. 29, 291–325.
[30] Brown, C.K., Madauss, K., Lian, W., Beck, M.R., Tolbert, W.D. and Rodgers, D.W. (2001) Proc. Natl. Acad. Sci. USA 98, 3127–3132.
[31] Oefner, C., D'Arcy, A., Hennig, M., Winkler, F.K. and Dale, G.E. (2000) J. Mol. Biol. 296, 341–349.
[32] Natesh, R., Schwager, S.L., Sturrock, E.D. and Acharya, K.R. (2003) Nature 421, 551–554.